A *BeppoSAX* observation of the X-ray pulsar 1E 2259+586 and the supernova remnant G109.1−1.0 (CTB 109)

A.N. Parmar[1], **T. Oosterbroek**[1], **F. Favata**[1], **S. Pightling**[2], **M.J. Coe**[2], **S. Mereghetti**[3], **and G.L. Israel**[4]

[1] Astrophysics Division, Space Science Department of ESA, ESTEC, P.O. Box 299, 2200 AG Noordwijk, The Netherlands
[2] Department of Physics & Astronomy, The University, Southampton SO17 1BJ, UK
[3] IFCTR, via Bassini 15, I-20133 Milano, Italy
[4] Osservatorio Astronomico di Roma, via dell'Osservatorio 1, I-00040 Monteporzio Catone, Italy

Abstract. The 7 s X-ray pulsar 1E 2259+586 and the supernova remnant (SNR) G109.1−1.0 (CTB 109) were observed by *BeppoSAX* in 1996 November. The pulse period of 6.978914 ± 0.000006 s implies that 1E 2259+586 continues its near constant spin-down trend. The 0.5–10 keV pulse shape is characterized by a double peaked profile, with the amplitude of the second peak $\sim$50% of that of the main peak. The pulse profile does not exhibit any strong energy dependence. We confirm the *ASCA* discovery of an additional low-energy spectral component from 1E 2259+586. This can best be modeled as a 0.44 keV blackbody, but we cannot exclude that some, or all, of this emission arises from the part of the SNR that lies within the pulsar's extraction region.

The spectrum of G109.1−1.0 is well fit with a non-equilibrium ionization plasma model with a best-fit temperature of 0.95 keV. The derived mass for the X-ray emitting plasma ($\sim$15–20 $M_\odot$) and its near cosmic abundances imply that the X-ray emission comes mainly from mildly enriched, swept-up circumstellar material. The spectrum is strongly out of equilibrium with an ionization age of only 3000 yr. This age is in good agreement with that derived from hydrodynamic simulations of the SNR using the above X-ray temperature.

Key words: stars: neutron – pulsars: individual (1E 2259+586) – ISM: individual objects: (G109.1−1.0) – X-rays: ISM – X-rays: stars

1. Introduction

1E 2259+586 is an unusual pulsar with a pulsation period of 7 s and a very steep spectrum (photon index, α, $\sim$4). The source has exhibited a near constant spin-down trend at $\sim$5$\times 10^{-13}$ s s^{-1} since its discovery. 1E 2259+586 is located in, or near, the supernova remnant (SNR) G109.1−1.0 which is also known as

CTB 109. The SNR consists of an approximately hemispherical shell of X-ray and radio emission and a jet-like lobe located mid-way between the shell and the pulsar (Gregory & Fahlman 1980; Hughes et al. 1981; Morini et al. 1988; Hurford & Fesen 1995). There may be a compact (2–3′ radius) synchrotron nebula surrounding the pulsar (Rho & Petre 1997). The location and shape of the X-ray lobe led to speculation that it is a "jet" of material connecting the pulsar and the SNR (Gregory & Fahlman 1983). However, its thermal spectrum and detailed morphology do not support this view (Hurford & Fesen 1995; Rho & Petre 1997).

1E 2259+586 together with other sources such as 1E 1048.1−593 and 4U 0142+614 belong to a small group of pulsars with similar spin periods (around 6 s) and properties that clearly distinguish them from the "classical" pulsars in high-mass X-ray binaries (Mereghetti & Stella 1995). Koyama et al. (1987) argue that the slow spin-down rate implies that 1E 2259+586 contains an accreting neutron star rotating at close to its equilibrium period with a magnetic field of $\sim$5 $\times 10^{11}$ G. However, there is no direct evidence that the pulsar is in a binary system. In particular, no optical or radio counterparts have been found (Coe & Jones 1992; Coe et al. 1994) and no Doppler shifts in pulse period have been detected (Koyama et al. 1989; Hanson et al. 1988; Morini et al. 1988).

The lack of an optical counterpart and orbital Doppler shifts argue against a binary models for 1E 2259+586, unless the companion has an extremely low mass. Models based on single stars have been proposed, such as spin-down of a white dwarf (Paczynski 1990; Usov 1994), loss of magnetic energy of a strongly magnetized neutron star (Thompson & Duncan 1993) and a neutron star accreting from a circumstellar disk (Corbet et al. 1995; van Paradijs et al. 1995). The detection by Mereghetti (1995) of a large change in the spin-down rate of the similar system 1E 1048.1−5937, as well as the long term pulse frequency fluctuations in 1E 2259+586 (Baykal & Swank 1996) support an accretion hypothesis.

We present a detailed study of the X-ray emission from 1E 2259+586 and G109.1−1.0 using the imaging capabilities
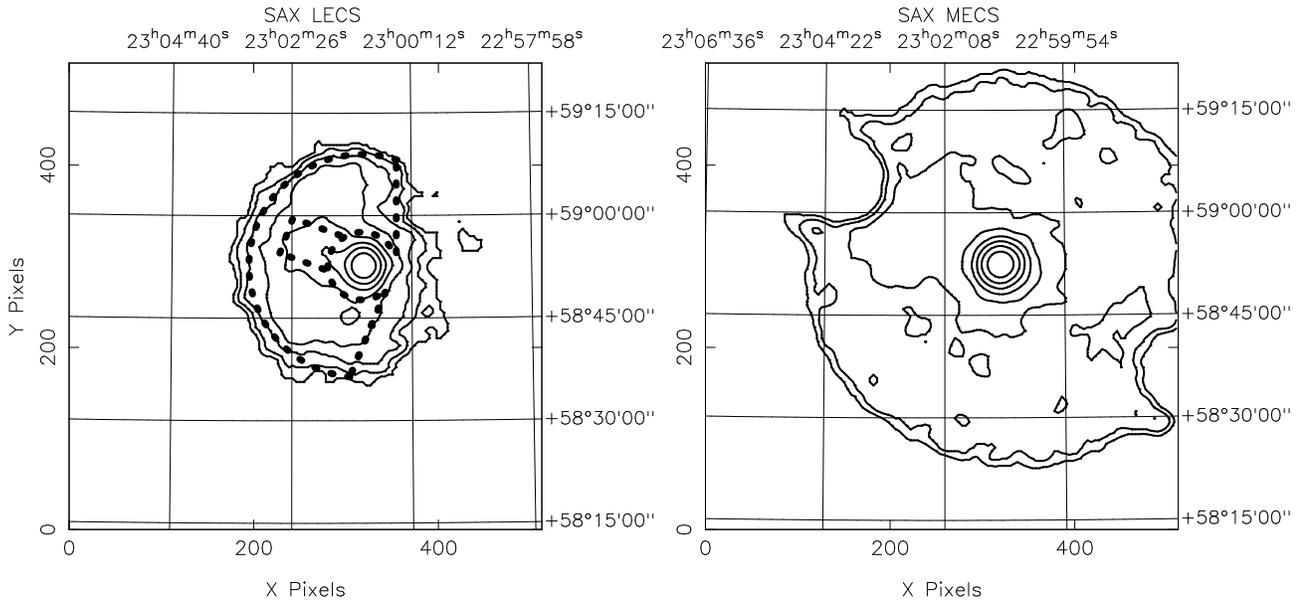
Fig. 1. LECS (left panel) 0.5–2.0 keV and MECS (right panel) 2.0–8.0 keV smoothed images of the region containing 1E 2259+586 and G109.1−1.0. The contours levels represent 1, 2, 3, 6, 12, 25 and 50% of the peak flux of each image. The "cut-outs" at the upper-left and lower-right of the MECS image are due to the removal of instrument calibration source events. The softness of the SNR and lobe can be seen by the greater asymmetry of the LECS contours, compared to the MECS. The extraction region used for the SNR shell spectrum is indicated by the heavy dotted line, minus the box shaped region (which is the extraction region for the lobe spectrum)

of *BeppoSAX* to separate the contributions of the individual sources. This topic is particularly interesting because of the disparate spectral results reported for 1E 2259+586 as well as of the uncertain origin of the X-ray lobe in G109.1−1.0.

2. Observations

Results from the the Low-Energy Concentrator Spectrometer (LECS; 0.1–10 keV; Parmar et al. 1997) and Medium-Energy Concentrator Spectrometer (MECS; 1.3–10 keV; Boella et al. 1997) on-board *BeppoSAX* are presented. The MECS consists of three identical grazing incidence telescopes with imaging gas scintillation proportional counters in their focal planes. The LECS uses an identical concentrator system as the MECS, but utilizes an ultra-thin (1.25 μm) entrance window and a driftless configuration to extend the low-energy response to 0.1 keV. The fields of view (FOV) of the LECS and MECS are circular with diameters of 37′ and 56′, respectively. In the overlapping energy range, the position resolution of both instruments is similar and corresponds to 90% encircled energy within a radius of 2′.5 at 1.5 keV. At lower energies, the encircled energy is proportional to $E^{-0.5}$. The LECS 0.1-10 keV background counting rate is 9.7×10^{-5} arcmin^{-2} s^{-1}.

The region of sky containing 1E 2259+586 and G109.1−1.0 was observed by *BeppoSAX* between 1996 November 16 03:32 and November 17 05:19 UTC. Good data were selected from intervals when the minimum elevation angle above the Earth's limb was >4° and when the instrument configurations were nominal using the SAXDAS 1.1.0 data analysis package. This gives exposures of 53.4 ks for the MECS and 15.2 ks for the

LECS, which was only operated during satellite night-time. The LECS and MECS images, smoothed using a Gaussian filter of width 1′.5, are shown in Fig. 1. 1E 2259+586 is visible as a point source close to the center of both images. The position of 1E 2259+586 derived by summing the LECS and the MECS data is 23$^{\rm h}$ 01$^{\rm m}$ 06$^{\rm s}$.8, 58° 52′ 16″ (J2000.0) with a 68% confidence uncertainty radius of 30″. This is consistent with the *Einstein* High Resolution Imager position of Fahlman et al. (1982). The SNR is visible as extended emission throughout both images.

Separate spectra were extracted for the pulsar, SNR shell and X-ray lobe regions. All spectra were rebinned to have >20 counts in each bin to allow the use of χ^2 statistics. Background subtraction was performed using standard blank field exposures.

3. Results

3.1. The 1E 2259+586 spectrum

LECS and MECS spectra were obtained centered on the pulsar position using an extraction radius of 4′. The 1E 2259+586 count rates above background are 0.28 and 0.55 s^{-1} in the LECS and MECS, respectively. Examination of the LECS spectrum reveals that the pulsar is only detected between 0.5 and 8.0 keV and data outside this range are excluded. Similarly, the MECS fit is restricted to the energy range 1.65–10 keV.

The combined LECS and MECS spectrum of the pulsar was first fit using a power-law model with $\alpha = 4.49 \pm 0.03$ and low-energy absorption of $(1.46 \pm 0.05) \times 10^{22}$ atoms cm^{-2} yielding a χ^2 of 449 for 266 degrees of freedom (dof). The photo-electric absorption coefficients of Morisson & McCammon (1983) and
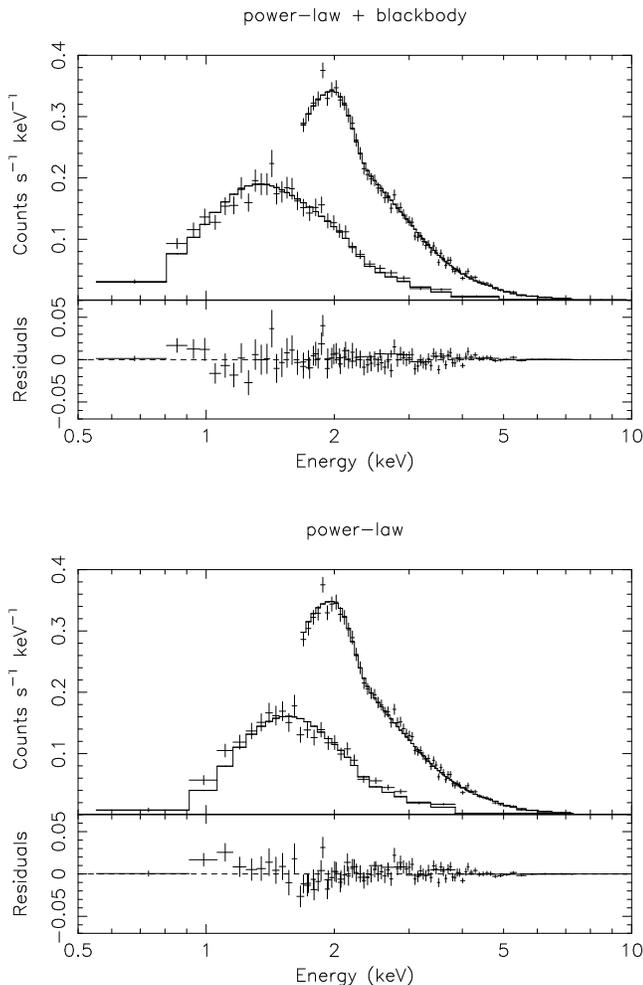
Fig. 2. The best-fit power-law and blackbody fit to the pulsar spectrum (top) and the best-fit power-law model fitted to the pulsar spectrum with 0.19 of the SNR shell spectrum subtracted (bottom). The smaller panels give the residuals in counts s^{-1} keV^{-1}. The models are described in the text and summarized in Table 1

Table 1. Spectral fit results for 1E 2259+586. Uncertainties are given at 68% confidence

Parameter	Value
Pulsar (power-law model)	
α	4.49 ± 0.03
N_H (10^{22} atoms cm^{-2})	1.46 ± 0.05
χ^2	449/266
Pulsar (power-law & blackbody model)	
α	3.93 ± 0.09
kT_{bb} (keV)	0.44 ± 0.01
Blackbody radius[a] (km)	$3.3^{+0.2}_{-0.3}$
N_H (10^{21} atoms cm^{-2})	8.7 ± 0.5
χ^2	271/264
Pulsar-0.19.SNR (power-law model)	
α	4.86 ± 0.04
N_H (10^{22} atoms cm^{-2})	2.18 ± 0.07
χ^2	296/265

[a]For a distance of 4 kpc

the solar abundances of Anders & Grevesse (1989) were used for all fits. Examination of the residuals reveals significant structure below ∼1.0 keV. A better fit (χ^2 of 271 for 264 dof) is obtained when a blackbody component is added. The spectral parameters listed in Table 1 are similar to those obtained using the same spectral model with *ASCA* spectra by Corbet et al. (1995) and with a combination of *ASCA*, *ROSAT*, and *BBXRT* spectra by Rho & Petre (1997). The remaining residuals near 1 keV may indicate an even more complex spectral shape.

In order to investigate an alternative explanation for the low energy residuals, the spectrum of the SNR shell multiplied by a scale factor, F, was subtracted from the 1E 2259+586 LECS spectrum (the SNR hardly contributes in the MECS energy range, see Fig. 4). The fit with a single power-law was then repeated and the best-fit value of F of 0.19 ± 0.01 determined by minimizing χ^2. This gives a χ^2 of 296 for 265 dof, and the amplitude of the residuals ≲1 keV is similarly reduced as with the power-law and blackbody fit (Fig. 2). The best-fit value of α is 4.86 ± 0.04 and N_H is $(2.18 \pm 0.07) \times 10^{22}$ atoms cm^{-2}. The ratio of the areas of the pulsar and SNR shell extraction regions (39 and 361 $arcmin^2$, respectively) is 0.11. This is comparable with the value obtained for F of 0.19, given the observed variations in surface brightness of the SNR, the presence of the X-ray lobe, and the extended (2–3′ radius) emission around 1E 2259+586 reported in Rho & Petre (1997). Although the fit quality is not as good as with the power-law and blackbody model, we cannot exclude the possibility that some, or all, of the residuals below ∼1 keV are caused by the contribution of the SNR that lies within the pulsar's extraction region. The 1E 2259+586 spectral fit results are summarized in Table 1. The 2–10 keV luminosity of 1E 2259+586 is 3.3×10^{34} erg s^{-1} for a distance of 4 kpc, identical to the value in Corbet et al. (1995).

3.2. 1E 2259+586 pulse timing and phase resolved spectroscopy

The MECS counts were used to determine the 1E 2259+586 pulse period, after correction of their arrival times to the solar system barycenter. The data were divided into 14 time intervals (each with ∼2000 counts) and for each interval the relative phase of the pulsations determined. This was performed by folding the counts at half the pulse period value, in order to obtain light curves with a stronger modulation. The phases of the 14 time intervals were then fitted with a linear function giving a best-fit period of 6.978914 ± 0.000006 s. The 1E 2259+586 light curve (Fig. 3) shows a double-peaked profile with the amplitude of the second peak about half that of the main peak.

A set of four phase-resolved spectra of the pulsar were accumulated, approximately coinciding with the peaks and valleys of the pulse profile. These spectra were fit with the same power-law plus blackbody model as used in Sect. 3.1, with N_H fixed at
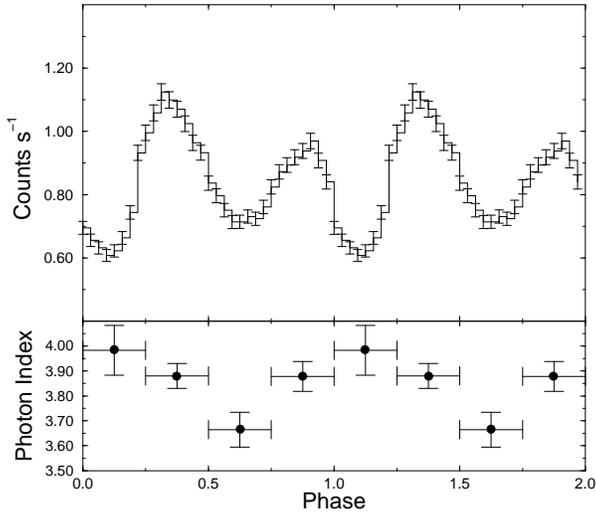
Fig. 3. The pulse profile (top panel) of 1E 2259+586 in the 0.5–10 keV energy range. The bottom panel shows the values of α. The values are repeated for clarity

Table 2. Spectral parameters for the one-component NEI fit to the SNR shell spectrum. Uncertainties are given at 90% confidence ($\Delta\chi^2 = 2.71$). A distance of 4 kpc is assumed. The X-ray lobe has consistent spectral parameters, except for an emission measure ($n_e \, n_H \, V$) of 27×10^{56} cm^{-3}

Parameter	Best-fit value	90% conf. range
N_H (10^{21} atoms cm^{-2})	6.9	5.7–7.6
kT (keV)	0.95	0.68–1.60
$n_e \, n_H \, V$ (10^{56} cm^{-3})	63	27–120
$n_e \, t$ (10^3 cm^{-3} yr)	1.2	0.7–2.4
[O/H]	2.0	0.5–5.0
[Ne/H]	1.1	0.0–1.2
[Mg/H]	2.4	1.3–3.9
[Si/H]	1.1	0.7–1.8
[S/H]	0.8	0.1–2.0
[Fe/H]	1.9	1.3–2.9

the phase-averaged best-fit value. There are insufficient counts to simultaneously constrain both the power-law and blackbody components. Initially, the blackbody spectral parameters were fixed at their phase-averaged best-fit values and only the power-law parameters allowed to vary. The fits were then repeated with the power-law parameters fixed while the blackbody parameters were allowed to vary. With the latter approach, the two fits in the valleys are unacceptable with χ^2_ν's of 2.9 and 2.3 for 117 dof. This is because the power-law component contributes too much flux, even if the contribution from the blackbody is set to zero.

The best-fit values of α obtained with the first approach are shown in Fig. 3 and reveal a small phase dependence. This variation corresponds to a χ^2 of 9.4 for 3 dof with respect to a constant value. Although this is significant at >99% confidence, we cannot be certain that there are real variations in α, since there is no clear correlation with the flux (as might be expected). In addition, small uncertainties in background subtraction, or a contribution from the SNR could cause such an effect, and so we prefer to set a limit of ± 0.2 to any phase-dependent change in α.

3.3. The G109.1−1.0 spectrum

In order to accumulate the spectrum of the SNR shell a complex shaped extraction region consisting of a circle, delimited by two straight lines with the pulsar and jet-like X-ray lobe cut out was used (see Fig. 1). Since the spectra of both the shell and the lobe are soft (there is little flux $\gtrsim 2$ keV), only LECS data were used. The effective area of the LECS depends on source position within the FOV and the appropriate response matrix was determined by using 11 point sources whose position and relative intensities were chosen to mimic the observed count distribution. Examination of the extracted spectrum shows that

the SNR is only detected between 0.25–4.5 keV and data outside this range are excluded.

The spectrum of the SNR shell was fit with the Non-Equilibrium Ionization (NEI) plasma emission model (plus absorption) implemented in V. 1.10 of the SPEX package. Fits were performed with freely varying O, Ne, Mg, Si, S, Fe and Ni abundances. A one-component NEI spectrum satisfactorily describes the spectrum with a χ^2 of 65 for 66 dof (see Table 2). The spectrum of the X-ray lobe was separately extracted and analyzed, using the region indicated in Fig. 1. Since the size of the extraction region is comparable to the standard LECS extraction region, no correction for source extent was applied to the response matrix. A background spectrum was obtained from the standard blank field exposures using the same extraction region as for the source spectrum. When the X-ray lobe spectrum is fit with the same NEI model, the best-fit values are in all cases within 1σ of those of the shell spectrum. This is in agreement with the results of Rho & Petre (1997) and supports the view that the two regions are physically related.

4. Discussion

The region of sky containing the 1E 2259+586 pulsar and the G109.1−1.0 SNR is complex. The 1E 2259+586 spectrum is best described by the sum of a power-law and a blackbody, confirming the results of Corbet et al. (1995). These authors suggest that at least part of the power-law component could originate from a synchrotron nebula which may be visible around 1E 2259+586 in *ROSAT* images (Rho & Petre 1997). A similar spectral decomposition has also been reported for two other "anomalous pulsars", 4U 0142+61 and 1E 1048.1−5937 (White et al. 1996; Corbet & Mihara 1997) and has been interpreted as evidence for quasi-spherical accretion onto isolated neutron stars after common envelope evolution and spiral-in (Ghosh et al. 1997). In this case the accretion flow has two components.
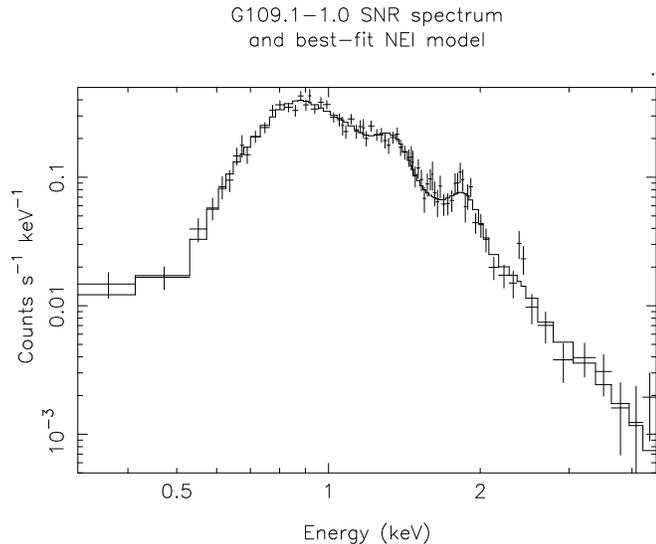
Fig. 4. The G109.1−1.0 shell spectrum, together with the best-fit single-component NEI model

Fig. 5. Pulse period history of 1E 2259+586. See Baykal & Swank (1996) for the measured values, except for the *BeppoSAX* result reported here

A low-angular momentum component giving rise to the blackbody emission from a large fraction of the neutron star surface, and a high-angular momentum one forming an accretion disk responsible for the power-law emission.

We caution that an alternative explanation for the observed two-component spectrum cannot be excluded for 1E 2259+586. If a plausible fraction of the emission arises from the part of the SNR within the pulsar's extraction region, then an acceptable fit can be obtained with a simple power-law model. This implies that the derived blackbody radius for 1E 2259+586 should be regarded as an upper limit. We note that with the power-law fit, the pulsar's N_H of $>2.1 \times 10^{22}$ atoms cm^{-2} is significantly greater than obtained for G109.1−1.0 of $<7.6 \times 10^{21}$ atoms cm^{-2}. This may indicate that the pulsar lies some distance beyond the SNR and that the two objects are unrelated, or it may indicate the presence of absorbing material local to the pulsar. The N_H to the SNR is consistent with the galactic column in the direction of 1E 2259+586 of 7.4×10^{21} atoms cm^{-2} (Dickey & Lockman 1990).

The derived pulse period is consistent with the extrapolation of the long-term spin-down measured by Corbet et al. (1995) and Baykal & Swank (1996) as can be seen in Fig. 5. No large change in spin-down rate, as observed for example from 4U 1626−67 (Chakrabarty et al. 1997), is evident. This implies that the accretion torque has remained approximately constant over at least the last 19 years.

In agreement with the results of Rho & Petre (1997), the LECS spectra of the SNR shell and of the jet-like X-ray lobe are indistinguishable, supporting a common origin for these two regions. We therefore refer to the summed spectrum as "the SNR". For an assumed distance of 4 kpc, the 15′ radius of the SNR shell corresponds to 17.5 pc, or an emitting volume of $f \times 6.6 \times 10^{59}$ cm^3, where f is the filling factor of the emitting plasma within a sphere. The mass of the SNR is then
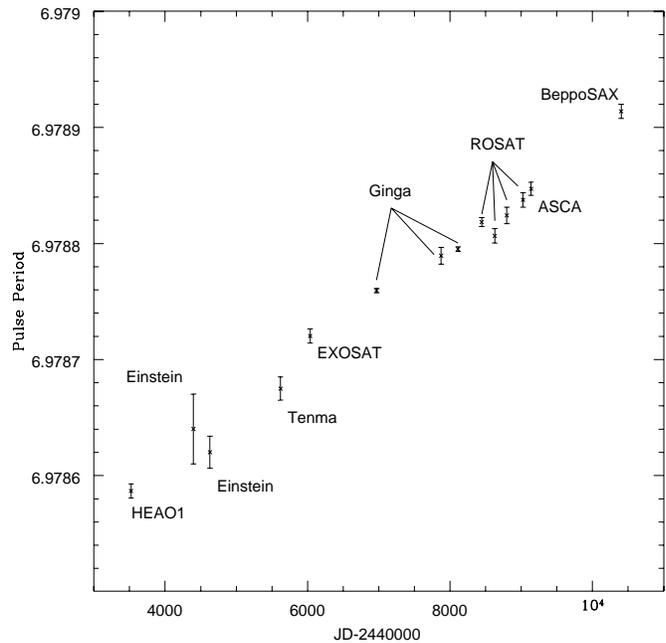
$60 \times f^{0.5}$ M$_\odot$. The canonical filling factor for a strong shock is 0.25, although the absence of half of the remnant reduces this by a factor of 2. The clumpiness of the X-ray emission (with most of the emission coming from a few bright spots) implies an even smaller filling factor, and we adopt a value of 0.1. The total emitting remnant mass is therefore ∼15–20 M$_\odot$. The remnant age is estimated to be 13,000 yr using the hydrodynamical model of Wang et al. (1992). However this estimate uses a remnant plasma temperature of 0.4 keV, significantly lower than determined here. The higher temperature implies a faster expansion speed (900 km s^{-1} rather than 590 km s^{-1}), and thus that the remnant is younger than previously estimated. The Wang et al. (1992) estimate is based on detailed numerical simulations, and it is not straightforward to determine the age corresponding to the updated temperature. Similarly, Hughes et al. (1981) determine an age of 17,000 yr assuming an X-ray temperature of 0.17 keV. Given their analytical approach, is possible to scale their estimated age to the current temperature determination to give a value of 3000 yr.

The low value derived for the emitting mass is consistent with a young remnant, which has not yet swept up large quantities of circumstellar material. The abundances derived from the X-ray spectrum are slightly higher than cosmic values, indicative of circumstellar material which has been mildly enriched either by the stellar wind of the progenitor in its late evolutionary stages, or by some moderate mixing-in of ejecta material. The value of the ionization parameter (1.2×10^3 cm^{-3} yr) is indicative of strong non-equilibrium conditions, with an implied ionization age of 3000 yr, in good agreement with the scaled numerical simulations of Hughes et al. (1981). The lack of strongly

enriched material implies that the ejecta is not being directly observed, and is also consistent with the lack of a strong wind of enriched gas originating from the progenitor in its late stages. This is suggestive of a low-mass progenitor and a Type Ib supernova.

The LECS fit results to the whole of the SNR are similar to those of Rho & Petre (1997), who analyzed BBXRT and *ROSAT* spectra of a small part of the remnant, just south of the pulsar. Their fit with a NEI model in non-equipartition also shows strong non-equilibrium conditions, with a comparable (considered the differences in the instrumental responses and plasma emission models) age of 6700 yr, near-cosmic or slightly enriched abundances and an emitting mass of 85 $M_\odot$.

References

Anders E., Grevesse N., 1989, Geochimica et Cosmochimica Acta 53, 197

Baykal A., Swank J., 1996, ApJ 460, 470

Boella G., Chiappetti L., Conti G., et al, 1997, A&AS 122, 327

Chakrabarty D., Bildsten L., Grunsfeld J.M., 1997, ApJ 474, 414

Coe M.J., Jones L.R., 1992, MNRAS 259, 191

Coe M.J., Jones L.R., Lehto H., 1994, MNRAS 270, 178

Corbet R.H.D., Smale A.P., Ozaki M., Koyama K., Iwasawa K., 1995, ApJ 443, 786

Corbet R.H.D., Mihara T., 1997, ApJ 475, L127

Dickey J.M., Lockman F.J., 1990, ARA&A 28, 215

Fahlman G.G., Hickson P., Richer H.B., Gregory P.C., Middleditch J., 1982, ApJ 261, L1

Ghosh P., Angelini L., White N.E., 1997, ApJ 478, 713

Gregory P.C., Fahlman G.G., 1980, Nat 287, 805

Gregory P.C., Fahlman G.G., 1983, in J. Danziger, P. Gorenstein (eds.), IAU Supernova Remnants and their X-ray Emission. Dordrecht, Reidel, p. 429

Hanson C.G., Dennerl K., Coe M.J., Davis S.R., 1988, A&A 195, 114

Hughes V.A., Harten R.H., van den Burgh S., 1981, ApJ 246, L127

Hurford A.P., Fesen R.A., 1995, MNRAS 277, 549

Koyama K., Hoshi R., Nagase F., 1987, PASJ 39, 801

Koyama K., Nagase F., Ogawara Y., et al., 1989, PASJ 41, 461

Mereghetti S., 1995, ApJ 455, 598

Mereghetti S., Stella L., 1995, ApJ 442, L17

Morini M., Robba N.R., Smith A., van der Klis M., 1988, ApJ 333, 777

Morisson D., McCammon D., 1983, ApJ 270, 119

Paczynski B., 1990, ApJ 365, L9

Parmar A.N., Martin D.D.E., Bavdaz M., et al., 1997, A&AS 122, 309

Rho J., Petre R., 1997, ApJ 484, 828

Thompson C., Duncan R.C., 1993, ApJ 408, 194

Usov V.V., 1994, ApJ 427, 984

Van Paradijs J., Taam R.E., van den Heuvel E.P.J., 1995, A&A 299, L41

Wang Z., Qu W., Luo D., McCray R., Mac Low M.-M., 1992, ApJ 388, 127

White N.E., Angelini L., Ebisawa K., Tanaka Y., Ghosh P., 1996, ApJ 463, L83